ISSN 0006-2979, Biochemistry (Moscow), 2025, Vol. 90, No. 11, pp. 1678-1697 © Pleiades Publishing, Ltd., 2025.
Published in Russian in Biokhimiya, 2025, Vol. 90, No. 11, pp. 1794-1815.

Relationships of *GDAP1* Mutations to Disease Phenotype and Mechanisms of Therapeutic Action of Oxidative Metabolism Activators in a Patient with Charcot–Marie–Tooth Neuropathy Type 2K

Nadejda R. Borisova[1], Alina A. Emelyanova[2], Olga N. Solovjeva[3], Natalia V. Balashova[4,5], Olga P. Sidorova[4], and Victoria I. Bunik[1,2,3,a]*

[1]*Sechenov University, 119048 Moscow, Russia*

[2]*Faculty of Bioengineering and Bioinformatics, Lomonosov Moscow State University, 119991, Moscow, Russia*

[3]*Belozersky Institute of Physico-Chemical Biology, Lomonosov Moscow State University, 119991 Moscow, Russia*

[4]*Faculty of Advanced Medicine, Vladimirsky Moscow Regional Research and Clinical Institute, 129110 Moscow, Russia*

[5]*Faculty of Continuing Medical Education, RUDN Medical Institute, 117198 Moscow, Russia*

[a]*e-mail: bunik@belozersky.msu.ru*

Received July 6, 2025
Revised October 5, 2025
Accepted October 18, 2025

Abstract—The development of personalized medicine, including the treatment of hereditary diseases, requires translation of advances in biochemistry into medical practice. Our work is dedicated to solving this problem in a clinical case of hereditary Charcot–Marie–Tooth neuropathy type 2K (CMT2K), induced by the compound heterozygous mutations in the *GDAP1* gene leading to the protein variants with the most common in Europe substitution L239F (inherited from the father) and previously uncharacterized substitution A175P (inherited from the mother). The ganglioside-induced differentiation-associated protein 1 (GDAP1) encoded by the *GDAP1* gene is located in the outer mitochondrial membrane and belongs to the glutathione S-transferase superfamily. Our structure-function analysis of GDAP1 shows that dimerization of its monomers with either L239F or A175P substitutions, along with the half-of-the-sites reactivity of GDAP1 to hydrophobic ligands, may synergistically impair the binding due to the double amino acid substitution in one of the active sites. This mechanism explains the early disease onset and progress in the child, whose parents heterozygous by each of the mutations are asymptomatic. Published phenotypes of amino acid substitutions in the GDAP1 region comprising the binding site for hydrophobic compounds are analyzed, including phenotypes of the homozygous L239F substitution and its compound heterozygous combinations with other substitutions in this region. Based on the found association of these substitutions with the axonal form of Charcot–Marie–Tooth disease (CMT) and disturbances in the NAD^+- and thiamine diphosphate (ThDP)-dependent mitochondrial metabolism, the therapeutic effect of nicotinamide riboside (NR) and thiamine (precursors of NAD^+ and ThDP, respectively) in the patient is studied. Oral administration of thiamine and NR increases levels of ThDP and NAD^+ in the patient's blood, improves the hand grip strength, and, after a long-term administration, normalizes the ThDP-dependent metabolism. After the therapy, the diseased-altered activities of transketolase (TKT) and its apo-form, as well as the relationship between the activity of the TKT holoenzyme and ThDP and NAD^+ levels in the patient's blood, approach those of healthy women. Our results demonstrate the therapeutic potential of thiamine and NR in correcting metabolic dysregulation in CMT caused by mutations in *GDAP1*, suggesting

* To whom correspondence should be addressed.

the underlying molecular mechanisms. Genetic diagnostics and biochemical characterization of mechanisms involved in the pathogenicity of mutations in clinically asymptomatic patients or patients at the early CMT stages may increase the efficacy of therapy, as it is easier to protect from the accumulating metabolic damage than to reverse it.

DOI: 10.1134/S0006297925601911

Keywords: GDAP1, pyruvate dehydrogenase kinase, compound heterozygous mutations, muscle strength, Charcot–Marie–Tooth neuropathy, nicotinamide riboside, thiamine, transketolase, tricarboxylic acid cycle

INTRODUCTION

Deciphering molecular mechanisms of pathologies caused by missense mutations is a challenge in personalized medicine [1]. Solving this problem is essential for developing patient-specific therapeutic interventions. In some cases, such as Charcot–Marie–Tooth disease (CMT), the pathological effects of missense mutations can develop asymptomatically over a long period of ontogenesis [2]. CMT is a very heterogeneous group of inherited motor and sensory polyneuropathies with a high incidence (1 : 2500) and autosomal dominant, autosomal recessive, and X-linked inheritance patterns [2]. Based on electrophysiological criteria, two major forms of CMT are considered, i.e., the demyelinating and axonal ones. X-linked subtypes are traditionally classified as a separate group CMTX. Early onset and severe progression might be associated with a mixed-type CMT, which is initially diagnosed as the axonal form [3]. In such cases, demyelination in the course of disease progression presumably results from continuous mitochondrial dysfunction, which usually induces axonal damage, representing a common biochemical feature of various neuromuscular diseases [4]. The clinical symptoms common for all CMT forms include progressive muscle weakness and muscle atrophy in lower limbs (especially, in distal regions), which later affect arms and proximal regions, as well as sensory loss, diminished tendon reflexes, and impaired nerve impulse generation and conduction [2].

Mutations in the ganglioside-induced differentiation-associated protein 1 (GDAP1), encoded by the *GDAP1* gene, are the fifth most frequent cause of the CMT in certain populations, leading to the development of its demyelinating, axonal, or mixed forms [2]. GDAP1 is highly expressed in neurons of the peripheral nervous system and Schwann cells (neuroglial cells involved in peripheral myelinogenesis) [5]. The clinical phenotypes of homozygous and compound heterozygous *GDAP1* mutations are characterized by early and significant impairments of predominantly motor functions that worsen with age. Depending on a particular *GDAP1* mutation (the number of known *GDAP1* mutations exceeds 80 [6]), the associated phenotypes range from very severe, diagnosed during the first year of life, to moderate, which develop over 2-3 decades [2, 3].

The effects of GDAP1 knockouts and knockdowns could vary depending on the experimental model. For example, disturbances in the mitochondrial morphology and calcium homeostasis detected in the GDAP1-deficient models correlate with a reduced number of contact sites between the mitochondrial and other cellular membranes (plasma membrane and membranes of the endoplasmic reticulum, lysosomes, and peroxisomes) [7-9]. Pleiotropic clinical and cellular phenotypes may be observed even for the same *GDAP1* mutations or their heterozygous combinations [10-16], suggesting that the cellular and organismal consequences of GDAP1 dysfunction depend on the context in which its molecular functions are realized. Unfortunately, these functions are characterized insufficiently.

According to the analysis of the amino acid sequence of GDAP1, this protein belongs to the glutathione S-transferase (GST) superfamily [17, 18]. Thus, GDAP1 contains domains homologous to the N- and C-terminal domains of GST, which include the glutathione-binding site and the hydrophobic-co-substrate-binding site, respectively (Fig. 1). Although the data on the glutathione binding and catalytic activity of GDAP1 in the GST reaction are contradictory [19-21], the ability of GDAP1 to bind hydrophobic compounds, such as etacrynic and hexadecanedioic acids, is demonstrated in independent studies [19, 20]. Furthermore, in patients with the CMT neuropathy type 2K (CMT2K), missense mutations in the GST domains of GDAP1 result in a faster disease progression compared to the missense mutations located outside of these domains, indicating the key role of the GST-homologous domains of GDAP1 in the CMT2K pathology [22].

In addition to the GST-homologous domains, GDAP1 contains the so-called α-loop within the C-terminal GST domain and two additional domains: the hydrophobic domain (HD) and the transmembrane (TM) domain (Fig. 1). The presence of extended α-loop,

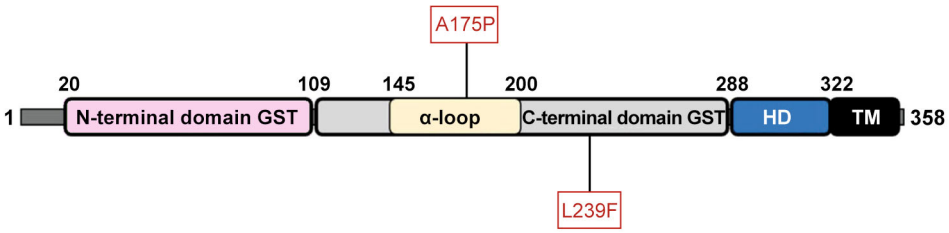

Fig. 1. Domain structure of GDAP1: pink, N-terminal GST domain containing glutathione-binding site; gray, C-terminal GST domain containing hydrophobic-co-substrate-binding site. Compared to the GST structure, the C-terminal GST domain in GDAP1 contains an insertion named the α-loop, most of which is not visualized in X-ray structures. Following the C-terminal GST domain, GDAP1 contains the hydrophobic domain (HD, blue) and the transmembrane domain (TM, black). Positions of mutations in GDAP1 of the studied patient are shown; the boundaries of the GDAP1 structural fragments are numbered according to [19].

which is largely unresolved in the GDAP1 crystal structures, is essential for GDAP1 dimerization, binding of hydrophobic compounds in the C-terminal GST domain, and formation of heterologous complexes with β-tubulin, Ras-related protein Rab-6B, and caytaxin (proteins involved in the vesicular transport) [19, 20, 23]. Another characterized property of GDAP1 is its membrane binding mediated by the C-terminal TM domain, which is important for the formation of contact sites between the mitochondria and other organelles, such as endoplasmic reticulum and lyosomes [9, 24]. Due to the influence of GDAP1 on the mitochondrial morphology, suggestions on its GTPase activity, similar to that of dynamin, have been considered, but neither the GTPase activity, nor the structural similarity of GDAP1 to GTPases have been found [19].

The aim of this study is to analyze the molecular basis of the pathogenicity of GDAP1 mutations, and of the therapeutic action of metabolic activators, in a female CMT2K patient with a compound heterozygous combination of two *GDAP1* missense mutations resulting in the amino acid substitutions L239F (with previously characterized clinical phenotype) and A175P (of unknown pathogenicity). The mutations are inherited from apparently healthy heterozygous father and mother, respectively. L239F is the most frequent GDAP1 mutation in the Central and Eastern Europe, whose pathogenicity is manifested in the homozygous state [15], while the pathogenicity of A175P and its combination with L239F remains unknown. To evaluate it, we integrate the results of our analysis of the structure-function relationships in the GDAP1 molecule with data on the clinical and cellular phenotypes of mutations in the *GDAP1* gene. Our findings suggest a negative impact of compound heterozygous L239F/A175P substitutions on the binding of hydrophobic compounds by GDAP1, which functions as a dimer with a half-of-the-sites reactivity for such compounds. Analysis of the patient's clinical phenotype and other known phenotypes associated with GDAP1 missense mutations affecting the hydrophobic ligand-binding region, reveals a common clinical picture of the axonal CMT neuropathy with the onset in the first decade of life. Based on the studies conducted in cells obtained from patients with *GDAP1* mutations altering the binding region for hydrophobic compounds, we predict the therapeutic effect of thiamine and nicotinamide riboside (NR) as precursors of the metabolic activators thiamine diphosphate (ThDP) and NAD^+, respectively. Consistent with the molecular mechanisms inferred from our analysis, administration of thiamine and NR improves and/or stabilizes the hand grip strength (typically decreased in CMT) and associated metabolic parameters, as demonstrated using a minimally invasive blood test. The use of dietary supplements therapy, similar to our administration of metabolic activators, attracts an increasing interest in the treatment of CMT [25].

MATERIALS AND METHODS

Reagents. Commercial reagents for biochemical assays were obtained from Helicon, Russia and were of the highest purity available. A mixture of pentose phosphates for the transketolase (TKT) activity assay was synthesized from ribose 5-phosphate using ribose 5-phosphate isomerase and xylulose 5-phosphate epimerase from bovine spleen acetone powder [26, 27]. Yeast TKT apoenzyme was isolated by immunoaffinity chromatography with polyclonal antibodies obtained from the serum of immunized rabbit according to the published protocol [28, 29]. The storage of TKT and its use in reactions have been described previously [30, 31]. Formate dehydrogenase for the NAD^+ assay was from Innotech MSU (Moscow, Russia).

Patient's clinical characteristics and medical history at the enrollment. The study was not preregistered. Prior to the study, written informed consent for participation in the study and publication of its results had been obtained from the mother

of the patient (a minor). The patient was diagnosed with CMT2K (an axonal form of hereditary motor and sensory CMT neuropathy) at the age of 7, based on clinical findings and genetic testing, which revealed two missense mutations in the GDAP1 gene in a compound heterozygous state: Ala175Pro (inherited from the mother) and Leu239Phe (inherited from the father). Both parents considered themselves healthy, while the absence of native GDAP1 protein in the child led to the early disease manifestation.

At the time of enrollment into the study at the age of 16, the patient presented with complaints of weakness in the legs and arms, slow gait, and inability to climb the stairs without support, rise from a squatting position, and stand on tiptoes or heels. Physical examination revealed muscle atrophy in the feet, lower legs, and hands (with interphalangeal joint contractures), as well as joint hypermobility with the Beighton score of 5. Hand grip strength was severely reduced to 5.1 kg in the right hand and 7.5 kg in the left hand, compared to the normal grip strength of ~26 kg for girls of the same age [32-34]. Tendon and periosteal reflexes in the upper extremities were moderately active; knee and ankle reflexes were absent. The patient experienced painful hypesthesia in hands and feet and maintained the Romberg position with difficulty due to weak legs, but accurately performed the finger-to-nose test. Vibration sensitivity in the toes was preserved.

Electroneuromyography at the time of enrollment showed a significant reduction in the amplitude of the compound muscle action potential and a less pronounced decrease in the conduction velocity of efferent (motor) fibers, particularly in the nerves of the lower limbs. The conduction velocity of afferent (sensory) fibers was at the lower limit of normal. The conduction velocity in the median nerve was 47-50 m/sec in both arms, which is above the threshold of 38 m/sec for diagnosing the demyelinating form of CMT, thus supporting the classification of this case as the axonal type [33]. However, ultrasound examination of nerves in the upper and lower limb revealed signs of altered nerve structure, suggesting demyelination.

Analysis of pathogenicity of the patient's mutations. For analysis, a structure of the GDAP1 dimer complex with a hydrophobic ligand (PDB ID: 7AIA [20]) was selected. To model the 3D structures of the α-loop, AlphaFold [35] as a general approach and PEP-Fold as a specialized approach to predict the spatial structures of short peptides up to 50 amino acid residues in length [36], were used. All structures were visualized with Pymol [37].

The 3D structures of proteins were shown as ribbon diagrams, and amino acid substitutions resulting from missense mutations were represented with ball-and-stick models. The regions present in both modeled and X-ray structures were superimposed using the Pymol align method [37]. The different conformations of the crystallographic structures of the dimer subunits in this region caused the differences in the superimposed regions and RMSD values of the superposition. For the subunit with the α-loop directed towards the hexadecanedioic acid molecule present in the crystal, these were the superimposed regions T147-G165 (N-terminal) and H199-D210 (C-terminal), with RMSD 4.578 Å. Similar superimposed regions for the α-loop of the other subunit of the dimer were T147-S162 and A184-N201, RMSD 6.162 Å.

Assessment of the effects of thiamine and NR on the clinical parameters. Thiamine (as thiamine hydrochloride) and NR were administered orally between the prescribed courses of neurometabolic therapy, which the patient received 2-3 times per year. These courses lasted 1.5 month each and included α-lipoic acid (Berlition 600 mg, intravenous infusion, or Thiogamma 600 mg, tablets), vitamin B12 (cyanocobalamin, 0.5 mg, intramuscular injection, or methylcobalamin, 1 mg, tablets), anticholinesterase agent ipidacrine (Axamon 5 mg, intramuscular injection or Axamon 20 mg, tablets), combined enzyme preparations (Wobenzym, 8 tablets per day), omega-3 polyunsaturated fatty acids, lecithin, and potassium iodide (Iodomarin, tablets).

During the course of thiamine and NR administration, the strength of the finger flexor muscles was measured regularly as a highly reliable and valid indicator of the CMT progression in adult patients [38, 39]. Standardized hand dynamometry with a DK-25 hand dynamometer (Russia) was performed as previously described [40].

Biochemical assessment of thiamine and NR effects. Whole blood samples were collected from the median cubital vein in the morning after an overnight fasting into heparin-containing vacuum tubes. The samples were frozen at −20°C and transported on ice to the laboratory, where the samples were stored at −70°C before being used in the experiments.

TKT activity in sonicated whole blood was measured spectrophotometrically at 340 nm from the absorbance of NADH produced in a coupled reaction using a CLARIOstar Plus microplate reader (Helicon, Russia) as described in [40]. The activity of TKT in the absence of ThDP corresponded to the activity of endogenous holo-TKT, which contains tightly bound, non-dissociating ThDP. The activity determined in the presence of ThDP was taken as the total TKT activity. The activity of endogenous apo-TKT lacking ThDP was determined as the difference between the total TKT activity and endogenous holo-TKT activity. Accordingly, the activation of TKT by ThDP added to the medium was calculated as [1 − (endogenous holo-TKT/total TKT)] × 100%.

ThDP content was measured in the extracts obtained from sonicated blood using a CLARIOstar Plus microplate reader in the spectrophotometric mode as described in [40]. The concentration of ThDP was determined enzymatically from the ThDP activation of yeast apo-TKT.

Blood NAD^+ content was determined in the methanol-acetic acid extracts prepared as described in [41] with modifications. After thawing, the blood was thoroughly mixed, and 30-µl aliquots were transferred to new microtubes. Next, 240 µl of ice-cold methanol was added to each tube. The blood-methanol mixture was sonicated with a Bioruptor (Diagenode; Liège, Belgium) in 3 cycles of 30 s each at the maximum power using ice cooling. After sonication, 40.5 µl of 2% acetic acid was added to each tube, and the samples were mixed on ice for 30 min in a New Brunswick Excella E24R incubator (Eppendorf, Russia) at 180 rpm. To remove denatured proteins, the extracts were centrifuged for 20 min at 21,500*g* at 4°C in a Hitachi CT15RE centrifuge (Helicon, Russia). The supernatants were transferred to clean tubes. The concentration of NAD^+ was measured enzymatically on the day of extract preparation based on the fluorescence of NADH formed in the reaction with formate dehydrogenase using a CLARIOstar Plus microplate reader according to the previously described protocol [41].

Female CMT patients and healthy women used in the study. For the correlation analysis, female participants (Table S1 in the Online Resource 1) were selected from a previously established database [40]. Parameters from young women of the age closest to that of the patient, were used as reference values.

Statistical analysis was performed using GraphPad Prism 8.0 (GraphPad Software, USA). The normal distribution of data was confirmed by the Shapiro–Wilk and Kolmogorov–Smirnov tests, and the correlation analysis for the cohorts was performed using the Pearson correlation coefficient. Multiple comparisons between the baseline values and NAD^+ content after thiamine and NR administration were performed using one-way ANOVA with the Tukey's *post hoc* test.

RESULTS

Prediction of effects of A175P and L239F substitutions on the structure and function of GDAP1. Deciphering molecular mechanisms of hereditary diseases caused by amino acid substitutions requires understanding the structure-function relationships in the protein molecule. Unfortunately, for many proteins, including GDAP1, such relationships are poorly characterized due to insufficient information on their molecular functions. This, in turn, is linked to difficulties in obtaining the full-length GDAP1 protein in a functionally active state regulated by natural mechanisms. Furthermore, the properties of various GDAP1 constructs studied in independent works differ significantly, depending on the structural parts removed to obtain a soluble protein and on the used expression system [19-21]. Nevertheless, the binding of hydrophobic compounds is a molecular function of GDAP1, established in independent studies using functional tests and crystallization. Essential structural prerequisites for the binding of hydrophobic ligands and strength of this binding are: the GDAP1 domain homologous to the C-terminal domain of GST, the GDAP1-specific α-loop within the C-terminal domain of GST, and the α-loop-facilitated dimerization of GDAP1 [19, 20]. Both patient's heterozygous GDAP1 mutations cause amino acid substitutions in these structural elements (Figs. 1 and 2a). Moreover, the substituted amino acids are strictly conserved in animals, from fish and amphibians to humans (Fig. S1 in the Online Resource 1), testifying to the functional importance of these residues.

In the structures of GDAP1 constructs resolved by X-ray analysis [monomer (PDB ID:6UIH) and dimers (PDB ID: 7AIA, 7YWD and 8EXZ) of the T157P mutant], L239 is identified in a loop region. The conformational mobility of such regions, as well as the location of the L239-containing loop in the vicinity of the hexadecanedioic-acid-binding site (Fig. 2a), support a contribution of L239 to the formation of the hydrophobic-ligand-binding site of GDAP1. The substitution of L239 with a bulkier phenylalanine residue as a result of mutation may impair such binding by altering both the binding pocket geometry and the hydrophobic interactions with surrounding residues, in particular, with neighboring C240, which plays an important role in maintaining GDAP1 stability [17].

In contrast to L239, A175 is located in a part of the α-loop that is not resolved in any of the published crystal structures of GDAP1, indicating multiple conformations and a high mobility of this region. Moreover, the visualized parts of α-loops in the subunits of the GDAP1 dimer (PDB ID: 7AIA) differ, depending on the hydrophobic ligand binding. That is, in the GDAP1dimer presented in Fig. 2a, the unresolved part of the α-loop of the upper subunit with the bound hexadecanedioic acid, comprises 22 residues (residues up to 162 and from 184 are visible), whereas in the ligand-free lower subunit, the unresolved part comprises 34 residues (residues up to 165 and from 199 are visible). The distances from the H'199 residue of the lower subunit to M116 (35 Å) and L239 (39 Å) in the ligand-bound site of the upper subunit are smaller than the distances from H199 of the upper subunit to the same residues in the lower subunit, i.e., M'116 (38 Å) and L'239 (46 Å). Remarkably, the GDAP1 dimer (PDB ID: 7AIA) with structurally

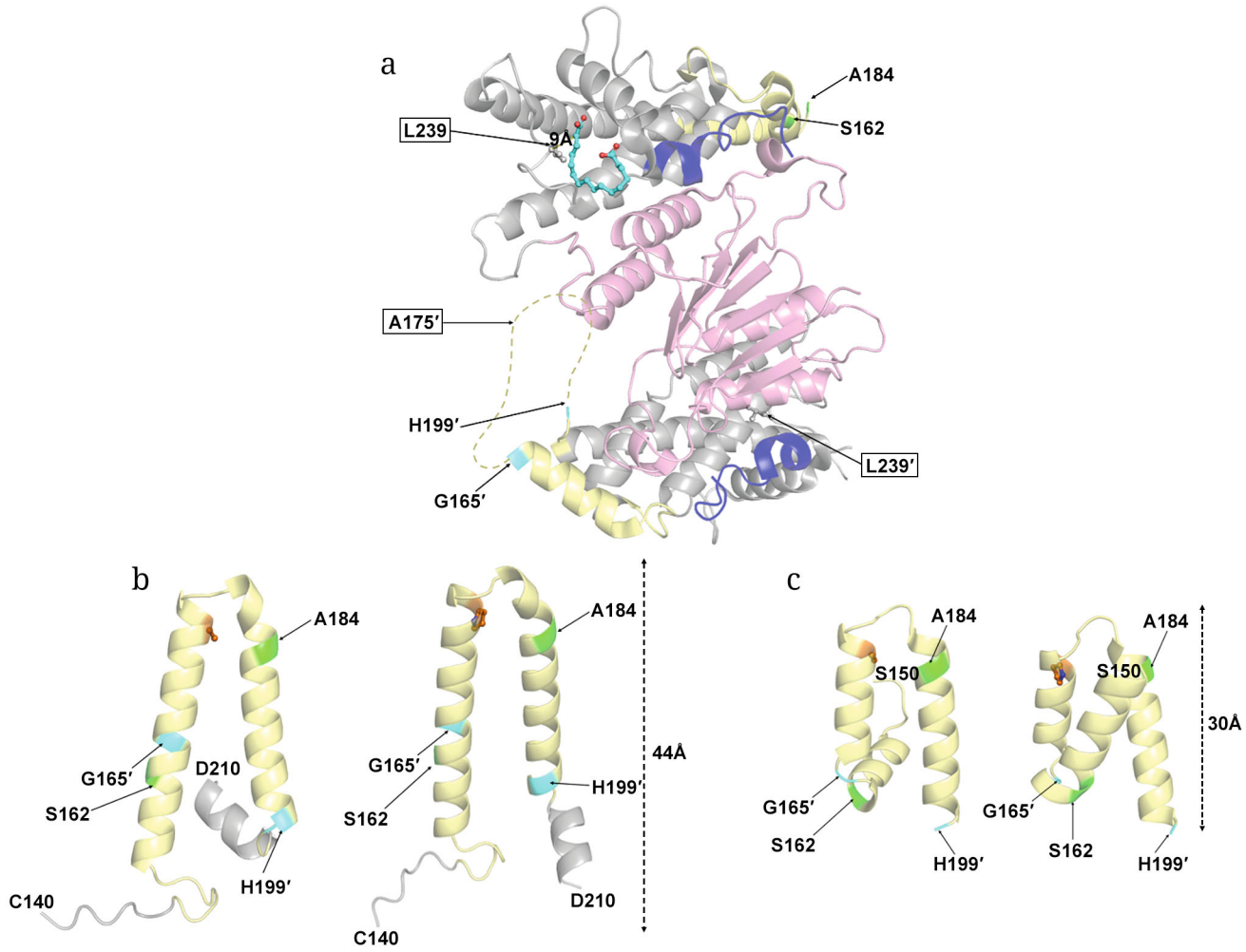

Fig. 2. Location of GDAP1 substitutions L239F and A175P in the hydrophobic-ligand-binding region (PDB ID: 7AIA). The terminal residues of the α-loop visualized in the dimeric X-ray structure are colored green for the upper subunit and light blue for the lower subunit (also labeled with a prime). **a)** Location of the GDAP1 α-loop and A175 and L239 residues substituted in the patient (framed), relative to the hexadecanedioic-acid-binding site in the GDAP1 dimer (PDB ID: 7AIA). **b)** Modeling of the GDAP1 α-loop structure and its flanking regions (residues 140-210) using AlphaFold. **c)** Modeling of the GDAP1 α-loop structure (residues 150-199) using PEP-Fold. Panels b and c show changes in the in silico modeled α-loop conformation caused by the A175P substitution (on the right) vs. the native peptide structure (on the left). The color code for the structural parts of GDAP1 is the same as in Fig. 1; in panels b and c, residue 175 (which is substituted in the patient's GDAP1) is shown in orange.

different α-loops binds the hydrophobic ligand in only one of the subunits, pointing to the half-of-the-sites reactivity of GDAP1 toward the hydrophobic ligand, which is associated with different conformations of its α-loops. The latter is confirmed by independent data on the significance of α-loop for the binding of hydrophobic compounds [19, 20]. These findings are consistent with the structure of the GDAP1 dimer presented in Fig. 2a, which implies dimer stabilization not only through the dimerization interface represented by the N-terminal GST domain (shown in pink), but also through the α-loop participation in the formation of the binding site for hydrophobic compounds, contributed by different subunits of the dimer. The high mobility allows one of the α-loops (α-loop of the lower subunit in Fig. 2a, whose unresolved structure is shown with yellow dotted line) to "close" the hydrophobic-ligand-binding site formed by the C-terminal GST domain of the other subunit (Fig. 2a). The length of the α-loop with (44 Å, Fig. 2b) or without (30 Å, Fig. 2c) its flanking regions, is comparable to the distance between H′199 at the bottom of the α-loop and L239 located near the hexadecanedioic acid (39 Å). Thus, the proposed involvement of the α-loop of one of the GDAP1 subunits in blocking the hydrophobic-compound-binding site of the other subunit, inferred from the GDAP1 dimeric structure (PDB ID: 7AIA; Fig. 2a), is confirmed both by the known role of the α-loop in enhancing the intersubunit contacts upon the hydrophobic ligand binding [19, 20] and by the

sensitivity of the α-loop conformation (residues 145-200, Fig. 1) to the binding of hydrophobic ligands (Fig. 2). The structure of the GDAP1 dimer presented in Fig. 2a suggests that the higher flexibility of the lower subunit α-loop (37 residues not visualized in the structure) compared to the more structured α-loop of the upper subunit (22 residues not visualized in the structure) is a manifestation of multiple α-loop conformations during its rearrangements required for closing the hexadecanedioic-acid-binding site, and a higher α-loop spiralization in the open conformation of the binding site.

Analysis of the GDAP1 X-ray structure (PDD ID: 7AIA; Fig. 2a) also reveals the proximity of the mobile α-loop (shown in yellow) to residues of the hydrophobic domain (shown in blue), which may ensure regulation of the α-loop conformation through its interaction with the hydrophobic domain participating in the autoinhibition of the GDAP1 GST activity [21]. The existence of structural premises for the α-loop interaction with the hydrophobic substrate required for the GST reaction, on one hand, and regulatory hydrophobic domain, on the other hand (Fig. 2a), is consistent with the results of independent functional studies on the α-loop involvement in the binding of hydrophobic ligands [19, 20] and autoinhibition of GST activity by the hydrophobic domain of GDAP1 [21].

The A175P substitution should significantly alter the spectrum of loop conformations due to (i) the greater stability of the *cis*-conformation of the peptide bond preceding the proline residue compared to the bonds formed by other amino acids, and (ii) proximity of the proline residues P175 (mutant) and P179. The differences in the conformations of the A175- and P175-containing loops are also confirmed by modeling the structures of GDAP1 peptides containing the native and substituted α-loops. Regardless of the program used and loop-flanking residues, the A175P substitution changes the peptide fold (Fig. 2, b, c). Although only the most stable structures with the *trans*-conformation of peptide bonds are modeled by default, in native proteins, peptide bonds between prolines and their preceding residues often have the *cis*-conformation [42]. Conformational changes caused by the *cis-trans* isomerization of such bonds are widely used in biological systems [43]. This factor may additionally influence the α-loop conformation induced by the A175P substitution and, accordingly, position of the loop relative to the hydrophobic-ligand-binding site.

Thus, the A175P substitution may alter the conformational spectrum of the α-loop involved in dimerization and binding hydrophobic compound in one subunit, while the L239F substitution may affect the same binding pocket for hydrophobic compound in its part formed by the other subunit (Fig. 2). As a result of the combination of the monomers with either L239F or A175P substitutions into the GDAP1 dimer, one of the binding sites of the dimer will get the double substitution. Hence, a greater dysfunction of this double-substituted binding site is expected, compared to the wild type and to the binding sites with the single substitutions L239F or A175P. Moreover, given the half-of-the-sites reactivity of GDAP1 towards hexadecanedioic acid considered above (Fig. 2a), impaired binding due to the amino acid substitutions in one binding site of the dimer will negatively affect the ligand binding in the other of the interacting sites. This mechanism can explain the dysfunction of GDAP1 in the patient with two heterozygous mutations in the absence of noticeable defects in the parents carrying single substitutions in GDAP1.

Common features of GDAP1 phenotypes induced by amino acid substitutions in the hydrophobic-compound-binding site. The structure–function analysis of GDAP1 conducted above shows that the A175P and L239F substitutions, which are not pathogenic in the heterozygous state (as in the parents at the time of study), may cause an early onset of pathology in the child due to a synergistic impairment in the GDAP1 binding of hydrophobic ligands. To get further evidence for this mechanism, available clinical and cellular phenotypes of GDAP1 mutations leading to substitutions in the protein regions within or near the hexadecanedioic-acid-binding site, have been analyzed (Table 1, Fig. 3). Because of the compound heterozygous state of GDAP1 mutations in the patient, Table 1 also includes the known phenotypes of compound heterozygotes of the widespread L239F substitution located in the studied protein region.

As can be seen from Table 1, all presented substitutions lead to the axonal type of CMT, i.e., affect generation of the nerve signal rather than the conduction velocity. The L239F substitution in the heterozygous state produces no clinical phenotype, while phenotypes resulting from the homozygous and compound heterozygous states of L239F are mainly characterized as moderate, with the onset during the first decade of life [15, 44-47]. The facts that the pathology caused by the compound heterozygous state of L239F was exacerbated to the level typical of homozygous replacements of residues in the region binding hydrophobic compounds, confirms the assumption about the critical role of hydrophobic ligand binding and subunit interactions in the dimer for the physiological function of GDAP1.

Given the progressive nature of CMT, its earlier onset maybe considered as a sign of a more severe phenotype. This occurs in patients carrying L239F in combination with mutations leading to the loss of arginine residues either near the hydrophobic-ligand-binding site (R282C) or in the region where α-loop interacts with the hydrophobic domain (R273G).

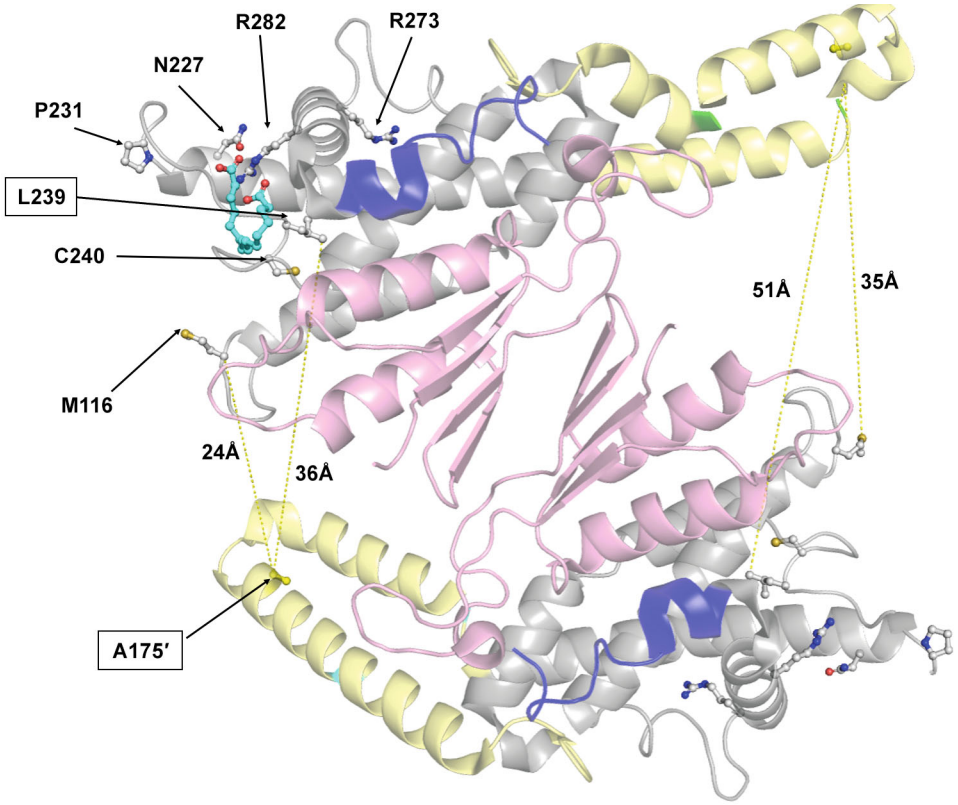

Fig. 3. Location of the GDAP1 amino acid residues substituted due to the mutations considered in Table 1, in the 3D structure of the GDAP1 dimer in complex with hexadecanedioic acid (PDB ID: 7AIA). The discussed residues are shown as ball-and-stick models in both subunits, but labeled only in the area of one hexadecanedioic-acid-binding site for better visualization. Residues of the lower subunit are marked with prime next to the residue abbreviation; residues substituted in the patient's GDAP1 are framed. The boundaries of the α-loop regions not visualized in the X-ray structure are indicated in light blue for the lower subunit (G165′ and H199′) and green for the upper subunit (S162 and A184). α-Loops modeled by AlphaFold (Fig. 2b) are superimposed by the Pymol align method, using the regions present in both X-ray and modeled structures. After that, the regions of the modelled α-loop, which correspond to those visualized in the X-ray structure of the dimer, are trimmed off.

In these cases, the disease onset shifts from the first decade to the first years of life (Table 1, Fig. 3). Moreover, the double substitution L239F/R273G, which potentially affects the regulatory interactions with the hydrophobic domain (Fig. 3), is associated with specific features of the clinical phenotype, such as hand tremor and hoarseness (Table 1).

According to ClinVar, the A175P substitution in GDAP1 is identified in germline cells, but neither its clinical phenotype is described, nor its pathogenicity and inheritance type are established (https://www.ncbi.nlm.nih.gov/clinvar/variation/657278/). The absence of pronounced symptoms of CMT in the heterozygous carrier of this mutation (patient's mother) indicates the absence of toxic action or significant dysfunction of GDAP1A175P, if the normal protein is synthesized from the other chromosome. The same applies to the synthesis of GDAP1 and GDAP1 L239F in patient's father. In contrast, the early onset of clinical symptoms in the compound heterozygous patient with both A175P and L239F substitutions in GDAP1 means strongly perturbed GDAP1 function, similar to that of the L239F homozygous state (Table 1). The similarity in the pathophysiological action of the A175P and L239F substitutions agrees with the results of our structure-function analysis, suggesting that both mutations affect the same molecular function of GDAP1, namely, the binding of hydrophobic compounds (Figs. 2 and 3).

Thus, amino acid substitutions in the hydrophobic-compound-binding site of GDAP1 lead to a common clinical phenotype of CMT, namely, its axonal form with the onset during the first decade of life. A combination of L239F with the substitutions affecting positive charges in the binding site or region adjacent to the regulatory hydrophobic domain, shifts the disease onset to the first year of life and may present additional clinical symptoms, as in the case of L239F/R273G substitutions (Table 1).

The most relevant models for elucidating the mechanisms underlying pathologies caused by protein variants are cells obtained from the patients

Table 1. Phenotypes of GDAP1 missense mutations within or near the hydrophobic-compound-binding site

Mutation	Clinical phenotype	Cellular models	References
A175P	No symptoms of CMT in an adult carrier of mutation in the heterozygous state	No data	This work
A175P/ L239F	Axonal type The disease begins at age 7. By age 16, weakness in the legs is accompanied by severe weakness in the arms and painful hypesthesia in hands and feet	No data	This work
P231L	Axonal type in homozygotes The disease onset in homozygotes is during the first years of life, with gradual progression. With age, the upper extremities become affected, and sensory impairment in the distal extremities develops [10, 11, 13]. Vocal cord paralysis and dysphonia may also occur [12]	No data	[10-13]
L239F	Axonal type in homozygotes The disease onset in homozygotes occurs during the first decade of life, primarily affecting the legs. Later, weakness and atrophy in the arms and mild sensory disturbances are observed. By the age of 20-30, some patients are forced to use a wheelchair [15, 45, 68]. Heterozygotes are asymptomatic	Expression of L239F GDAP1 in HeLa cells with low GDAP1 expression affects morphology of the Golgi apparatus and reduces the level of endogenous GDAP1 expression [69]. Structural data suggests decreased stability of GDAP1with this substitution [17]	[15, 17, 45, 68, 69]
L239F/ M116T	Axonal type Onset at 5-10 years of age [15]	M116R GDAP1 does not differ from the wild-type protein in its ability to protect against glutamate toxicity in HT22R cells [16] or to induce mitochondrial fragmentation in COS7 cells [5]	[5, 15, 16]
L239F/ N227D	Axonal type Onset at 4-10 years of age [15]	No data	[15]
L239F/ R273G	Axonal type Onset at 2 years of age. Hand tremors, hoarseness [15]	Comparison of motor neurons obtained from pluripotent stem cells of healthy control and a patient with compound heterozygous L239F/R273G mutation shows that the substitutions in GDAP1 decreased mitochondrial Ca^{2+}, increased PDH phosphorylation, increased glutamate dehydrogenase activity, and decreased glutamate level [14]. In the patient's fibroblasts, expression of GDAP1 mRNA and protein is significantly reduced, the glutathione level is reduced by 40%, and the mitochondrial potential decreases by 30%, compared to the control fibroblasts [16]	[14-16]
L239F/ R282C	Axonal type Onset at 2-3 years of age [15]	No data	[15]

Table 1 (*cont.*)

Mutation	Clinical phenotype	Cellular models	References
C240Y	Axonal type in heterozygotes The ages of three studied patients, all carrying mutation in the heterozygous state, ranged from 48 to 78 years. Sensory nerve potentials were not recorded, while motor nerve potentials and conduction velocity were normal. Reflexes in the lower extremities were absent, and tactile hypesthesia of the sock-glove type was observed. Chronic denervation in the upper extremities was present without histological abnormalities in muscle biopsy specimens. In contrast to the predominant motor impairment of the distal segments' characteristic of CMT, weakness of the proximal segments of the legs was observed; foot deformity characteristic of CMT was absent [22, 48]	The lactate to pyruvate ratio in the culture medium of fibroblasts from patients heterozygous for the C240Y mutation in GDAP1 increases to 12-22, while the control values are 4-12. In the patients' fibroblasts, the rate of mitochondrial respiration and oxidative phosphorylation on pyruvate/malate, activity of complex I of the electron respiratory chain, and activity of aconitase are reduced by 40-50%. Expression and composition of complex I, activities of citrate synthase and fumarase, and the ratio of isocitrate dehydrogenase to citrate synthase are not significantly changed by the substitution. The level of reactive oxygen species is increased; the expression of sirtuin 1 is reduced, while the expression of sirtuin 3 remains unchanged in cells with the C240Y substitution (vs. C240 in wild-type GDAP1). The size and mass of tubular mitochondria are increased by 33 and 20%, respectively [22, 48]	[22, 48]

Note. Mutations identified in the patient are shown in bold italic. Common symptoms of the developed CMT typically include weakness, decreased tendon reflexes, and muscle atrophy (predominantly in the lower limbs), deformity of the lower extremities (bilateral hollow foot), and gait impairment.

possessing these protein variants, since in such cells the native and/or substituted proteins function within the metabolic networks, which are not externally manipulated. Due to the limited availability of such cells for scientific research, in particular, because of the rare occurrence of specific GDAP1 mutations, inference from available published data is particularly important for the development of personalized medicine. The results of our analysis presented in Table 1 show that despite different sets of indicators used in independent studies, a common feature of patients' cells expressing GDAP1 with substitutions affecting the hydrophobic-compound-binding site, is altered mitochondrial metabolism. In particular, the oxidation of pyruvate in the tricarboxylic acid (TCA) cycle is changed. That is, motor neurons differentiated from pluripotent stem cells of a patient with the compound heterozygous L239F/R273G mutations demonstrate a number of interrelated changes, such as decreased mitochondrial Ca^{2+}, increased phosphorylation of α-subunit of pyruvate dehydrogenase (PDHA), increased level of glutamate dehydrogenase and decreased glutamate content [14]. Patient's fibroblasts with the compound heterozygous L239F/R273G mutation show decreased mitochondrial potential and reduced glutathione level, along with a significant downregulation of the endogenous GDAP1 expression [16]. Cultured fibroblasts from a patient with the substitution of a residue next to L239, i.e., C240Y, exhibit an increased lactate/pyruvate ratio in the culture medium, 40% reduction in the mitochondrial respiration on pyruvate/malate, 40% reduction in the mitochondrial complex I activity, and 50% decrease in oxidative phosphorylation [22, 48]. In contrast to the C240Y substitution, the R120W substitution outside the hydrophobic-compound-binding site causes no significant increase in the lactate/pyruvate ratio [22]. According to an independent classification [49], the lactate/pyruvate ratio <25 observed in the studied cells (Table 1) usually indicates deficient PDH function, whereas the lactate/pyruvate ratio >25 indicates insufficient activities of pyruvate carboxylase, TCA cycle, and respiratory chain.

Thus, the studies in cells from patients with mutations leading to the amino acid substitutions in the hydrophobic-compound-binding region of GDAP1 show that such substitutions are associated with increased PDH phosphorylation and reduced mitochondrial oxidation of pyruvate and NADH. ThDP is an inhibitor of PDH phosphorylation and, simultaneously,

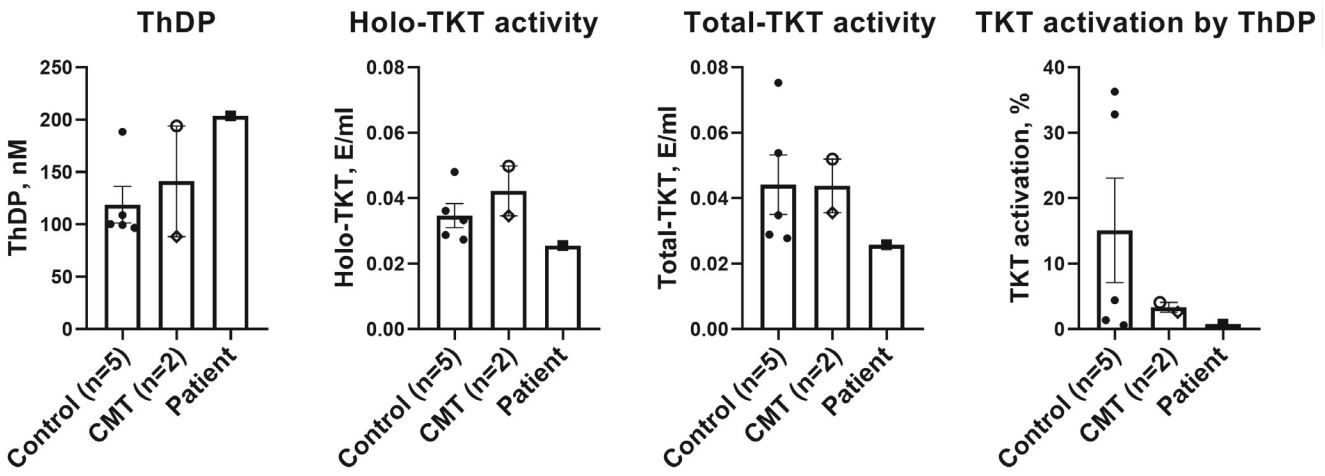

Fig. 4. The thiamine status of the CMT2K patient compared to young healthy women and young female patients with other forms of CMT (CMT1A and CMTX1). All parameters are presented as mean ± standard error of mean (SEM).

a coenzyme activating dephosphorylated PDH [50, 51]. Hence, the ThDP precursor thiamine may have a therapeutic effect in the studied patient having the hydrophobic-compound-binding region of GDAP1 impaired by the L239F/A175P substitutions. On the other hand, association of the GDAP1 substitutions in the hydrophobic-compound-binding region with the reduced PDH function indicates that the substrate flux through the TCA cycle is decreased in the patient. In a number of pathologies, an NAD^+ precursor NR not only activates the TCA cycle, but also improves the exercise tolerance [52-54]. Based on these observations, the ability of NR along with thiamine to correct the metabolic dysfunction in the patient with the L239F/A175P substitutions has been tested.

Patient's thiamine and NAD^+ status before the therapy. The assessment of the thiamine status of an individual is based on the determination of blood levels of the major intracellular form of thiamine, the coenzyme ThDP, as well as the activity and coenzyme saturation of the ThDP-dependent enzyme TKT [40]. Based on these parameters, we found no thiamine insufficiency in the patient's blood compared to other young women, either without or with CMT (Fig. 4). Before the thiamine administration, the ThDP level in the patient's blood (200 nM) corresponds to the upper limit in the control group. In contrast to ThDP, the TKT activity in the patient's blood is at the lower limit of the normal range, i.e., approximately two-fold lower than the average TKT activity in other young women, either without or with CMT (Fig. 4). Furthermore, no ThDP activation of TKT in the patient's blood is observed upon the ThDP addition to the reaction medim, while in the control group, TKT is activated by ThDP (Fig. 4). A relatively low TKT activity and the absence of ThDP-induced TKT activation in the patient's blood are the features previously established in the CMT patients [40]. In particular, both the TKT activity in the blood and its activation by ThDP are decreased at the disease advanced stages [40], which in the case of GDAP1 mutations are observed in the first decades of life. As a result, the thiamine status of the studied patient is consistent with the published results, indicating the absence of thiamine deficiency in CMT patients and the marker role of the blood TKT activity and TKT regulation by ThDP in the CMT pathology [40].

The concentration of NAD^+ in the patient's blood (6-7 μM) is significantly lower than in the control (15-23 μM) and neurological group (13-16 μM) [41]. Such low NAD^+ level may be associated with a much earlier disease onset in the case of GDAP1 mutations, suggesting a rapid development of pathology, compared to the previously studied patients with other forms of CMT starting in the 4th-5th decades of life. Indeed, the blood NAD^+ content shows a trend to decrease in cardiology patients with stage 3 of heart failure, compared to those with stage 2 [41].

Effects of mitochondrial metabolism activators on the hand grip strength, ThDP and NAD^+ levels, and TKT activity in patient's blood. The therapeutic effects of thiamine and NR were studied between the courses of neurometabolic therapy, alongside daily administration of L-carnitine at a dose of 500 mg. The patient received thiamine hydrochloride orally at a daily dose of 100 mg for the first 2 months, followed by 100 mg every other day for the next 4 months. Starting from the 3rd month, NR was added at a daily dose of 100 mg and from the 6th month – at the same dose every other day.

Daily oral administration of thiamine hydrochloride at a dose of 100 mg increases the ThDP blood level, while reducing the dose to 100 mg every other day decreases it (Fig. 5a). Similar effects are observed

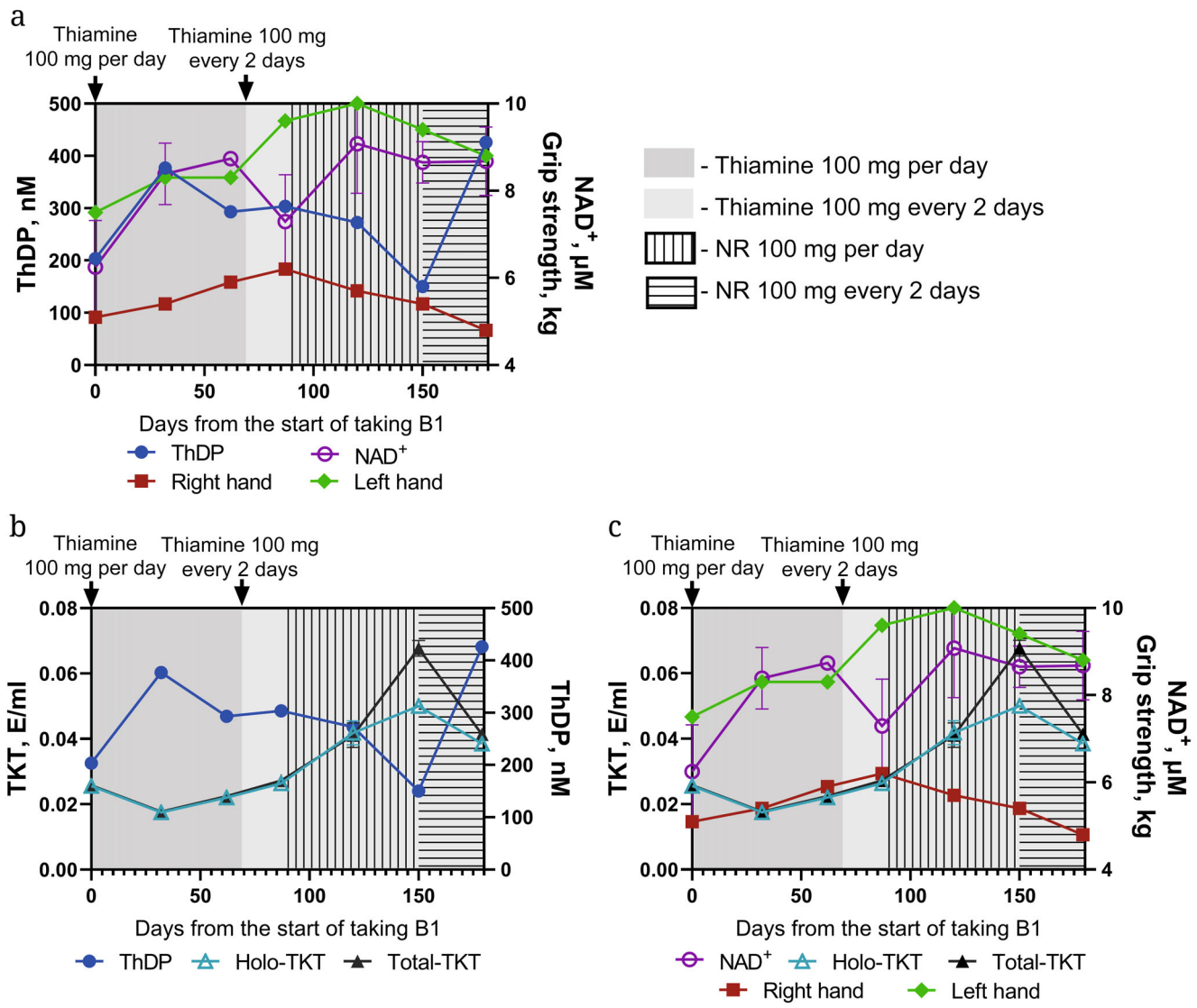

Fig. 5. Effect of oral administration of thiamine and NR on the blood levels of ThDP, NAD^+, TKT and on the hand grip strength. a) Changes in the hand grip strength and the blood ThDP and NAD^+ concentrations. b) Changes in the blood TKT activity and ThDP content. c) Changes in the hand grip strength and blood TKT activity and NAD^+ content. All biochemical parameters are presented as mean ± SEM (error bars are not seen if within the symbol size).

for the hand grip strength: daily thiamine administration increases it, while administration of the same dose every other day leads to a gradual decrease in the grip strength compared to the maximum value observed during the daily administration (Fig. 5a).

The dynamics of changes in the blood ThDP levels upon thiamine administration (Fig. 5a) has a non-monotonous pattern and demonstrates a delayed effect of thiamine administration on the hand grip strength, compared to changes in the blood ThDP concentration. That is, the peak of the blood ThDP concentration is observed after one month of daily thiamine intake. After that, the level of ThDP decreases even with the same vitamin B1 dosage, and remains stable after the dose has been reduced from 100 mg per day to 100 mg every two days. Throughout this period, the hand grip strength of both right and left hands gradually increases. Compared to the blood ThDP levels, the changes in the grip strength are more monotonous, which is likely related to the buffering capacity of tissues for thiamine and increase in this capacity in response to a higher thiamine availability, for instance, due to the altered tissue-specific expression of proteins of thiamine metabolism. Presumably, the blood ThDP concentration is influenced not only by adaptations of blood cells to a high thiamine availability, which stabilizes its level and resulting blood metabolism, but also by the overall saturation of tissues with thiamine delivered by the blood. The influence of these factors is consistent with the observed non-monotonous changes in the

ThDP content and metabolism in the blood, as well as by the delayed effect of thiamine on the hand grip strength, compared to the blood ThDP levels (Fig. 5a).

The regulatory significance of thiamine for central metabolism is evident from changes in the blood levels of another coenzyme – NAD^+. Even with the thiamine administration alone, i.e., without additional supplementation with the NAD^+ precursor NR, the content of NAD^+ increases simultaneously with the increase in the ThDP levels (Fig. 5a). After one and two months of daily thiamine intake, the blood levels of NAD^+ become significantly higher ($p < 0.04$) than those observed initially. Reducing the thiamine dose by switching from a daily regimen to every other day administration decreases the NAD^+ levels, but not the ThDP content (Fig. 5a). However, the following administration of the biosynthetic NAD^+ precursor NR alongside thiamine changes the positive relation between the ThDP and NAD^+ levels observed upon taking thiamine alone, to a negative one. Specifically, combined administration of thiamine (100 mg every other day) and NR (100 mg daily) expectedly increases the NAD^+ level compared to the initial one ($p < 0.03$). However, under these conditions, the increase in the NAD^+ content is accompanied by the decrease in the ThDP level (Fig. 5). Reducing the dose of NR to 100 mg every other day while maintaining the same thiamine dosage, stabilizes the NAD^+ level and increases the level of ThDP (Fig. 5). Both thiamine and NR are imported by the cells via specific transporters [55, 56]. However, at high doses, the uptake of these organic cations or their metabolites could also involve other proteins, such as organic cation transporters (OCTs) [56, 57]. The competition for transporters may contribute to the observed negative correlation between the ThDP and NAD^+ levels during combined administration of thiamine and NR. On the other hand, the positive correlation between the ThDP and NAD^+ levels observed when thiamine is administered alone, may reflect an improvement in the body's biosynthetic capacity due to the thiamine-dependent normalization of metabolism.

Comparison of changes in the hand grip strength and blood ThDP or NAD^+ levels (Fig. 5a), shows a greater correlation of the grip strength with the levels of ThDP than those of NAD^+. When the ThDP content is increased by thiamine administration, the muscle strength of both right and left hands increases, while subsequent decrease in the ThDP content upon the dosage reduction is paralleled by a decrease in the hand grip strength. In contrast, the decrease in the blood NAD^+ levels after reducing the thiamine dose does not affect the increase in the hand grip strength, while increase in the blood NAD^+ levels caused by NR administration does not prevent decreases in the hand grip strength (Fig. 5a).

Given a previously demonstrated role of blood TKT as an indicator of pathological metabolic changes in CMT patients [40], the association of the blood ThDP-dependent TKT activity with the intake of thiamine and NR has been investigated in the patient. Figure 5b shows that the blood TKT activity decreases with the increase in the blood ThDP content and, vice versa, increases with the ThDP decrease. At the same time, thiamine administration alters the activities of both total and holo-TKT to a similar extent, without causing significant changes in the ThDP-induced TKT activation (Fig. 5b). However, a combined intake of thiamine and NR, which decreases the blood ThDP level, increases the ThDP-induced TKT activation (Fig. 5b). Importantly, blood ThDP itself is not the only determinant of the TKT activation, i.e., even if the blood ThDP levels in the initial state and after the combined intake of thiamine and NR are the same, the activation of TKT by the coenzyme is observed only in the latter case (Fig. 5b). Reducing the NR dose upon continuous thiamine administration increases the blood ThDP levels, that results in the disappearance of the ThDP-induced TKT activation. The appearance of the ThDP-induced activation of the blood TKT (Fig. 5b), which is a sign of normal metabolism and is almost absent in CMT (Fig. 4) [40], indicates normalization of the patient's metabolism as a result of combined administration of thiamine and NR. However, changes in the blood TKT and hand grip strength do not correlate, similar to those in the grip strength and blood NAD^+ (Fig. 5c).

Therefore, the patient's TKT activity and blood ThDP levels show an inverse relationship, and administration of 100 mg/day NR upon the thiamine intake of 100 mg every other day promotes metabolic normalization, assessed by the activation of blood TKT by ThDP (Fig. 5).

Analysis of correlation between the blood NAD^+ levels and parameters of thiamine status in healthy women and female patients with CMT. Our results on the separate and combined intake of thiamine and NR by a patient with CMT2K has revealed novel patterns of interaction between the blood levels of NAD^+ and ThDP or TKT activity (Fig. 5). Taking into account previously established sex differences in the thiamine metabolism [40], correlations between the blood levels of NAD^+ and thiamine status parameters (ThDP, TKT activity) have been examined, using available samples of women without and with CMT. Comparison of correlations between the blood levels of NAD^+, ThDP, and holo-TKT activity in these samples (Fig. 6) shows that healthy women exhibit a negative correlation between the blood levels of NAD^+ and ThDP ($Rp = -0.58$, $p = 0.06$). The positive character of this correlation in the female CMT patients ($Rp = 0.75$, $p = 0.03$) points to metabolic changes associated

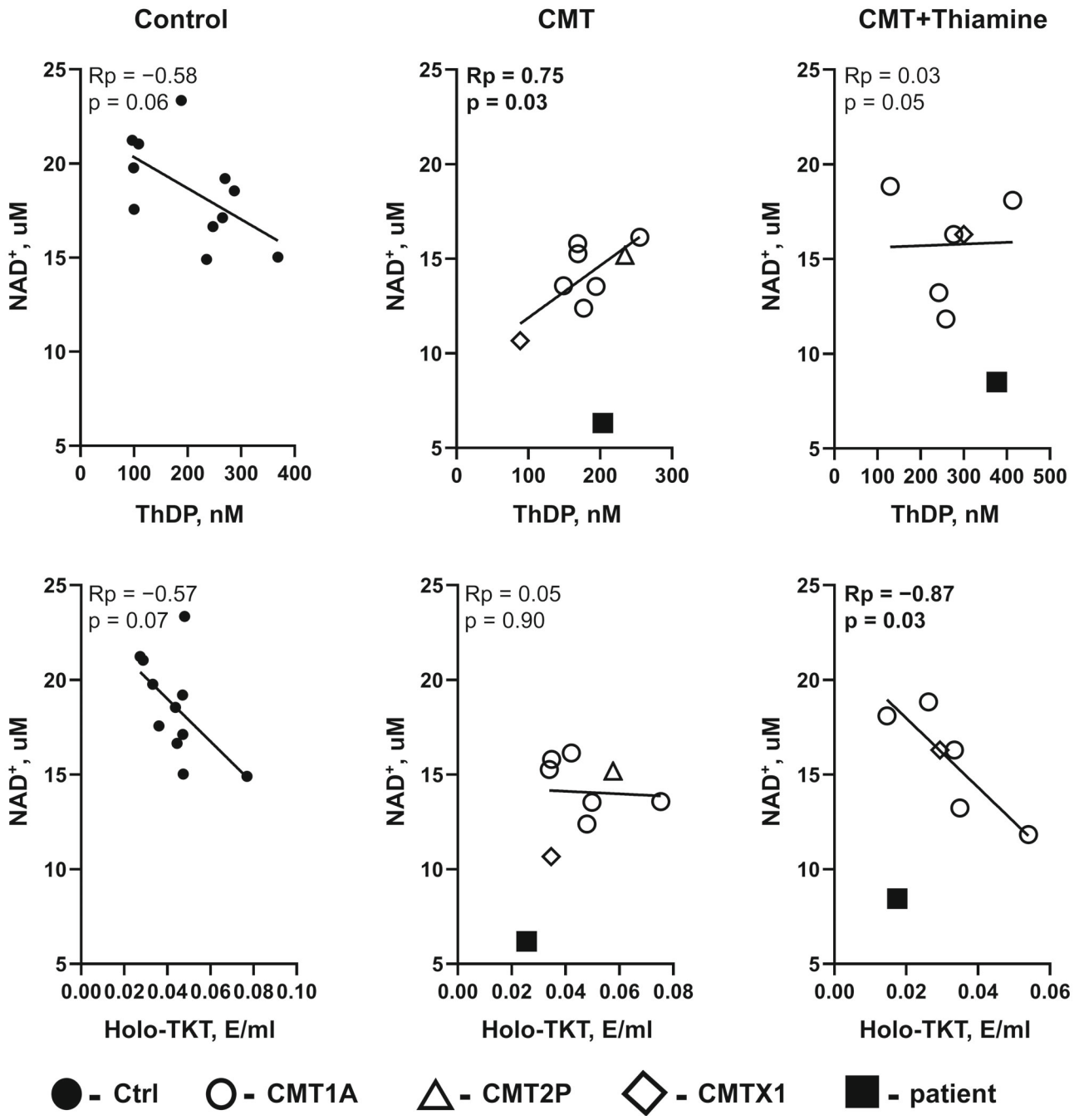

Fig. 6. Correlations between the NAD^+ levels and thiamine status parameters in the blood of healthy women (control, n = 11) and female CMT patients before (n = 8) and after 1-3 months of thiamine supplementation (n = 6). Pearson coefficients (R_p) and significance values (p) of the correlations are shown on the graphs; significant correlations ($p < 0.05$) are marked in bold. The data for different CMT forms are indicated by different symbols according to the legend. Abnormally low NAD^+ values of the CMT2K patient investigated in this work (with the disease onset during the first decade of life), compared to other patients (CMT1A and CMTX1, with the disease onset during the 4th-5th decade of life), are not included in the correlation analysis.

with the disease. During the initial stage of thiamine intake by the CMT2K patient (Fig. 5a, first month of thiamine administration), the relation between the blood levels of NAD^+ and ThDP is also positive. Hence, the direction of correlation between the blood levels of NAD^+ and ThDP is different in the affected (positive correlation) and healthy (negative correlation) women.

As a result of thiamine administration, the correlation coefficient between the NAD^+ and ThDP levels in female CMT patients decreases from 0.75 to 0.03 (Fig. 6). The disappearance of the positive correlation

suggests a therapy-induced shift from the positive relationship between the NAD^+ and ThDP levels, characteristic of CMT patients (R_p = 0.75), towards the negative correlation typical for healthy women (R_p = −0.58). This transition is presumably facilitated by the combined administration of thiamine and NR, since under these conditions, the blood levels of NAD^+ and ThDP in the CMT2K patient show the opposite changes (Fig. 5), corresponding to the negative correlation of these parameters in healthy females (Fig. 6, control). Similarly, a significant negative correlation between the blood levels of NAD^+ and endogenous holo-TKT activity, which is observed in healthy women and disappears in the CMT female patients, is restored after the thiamine therapy (Fig. 6). In the case of CMT2K patient, the increase in the NAD^+ content upon combined administration of thiamine and NR decreases the level of endogenous holo-TKT activity from 94 to 74% of the total TKT activity (Fig. 5b), which corresponds to the negative correlation between the blood levels of NAD^+ and TKT activity observed in healthy women (Fig. 6).

Thus, the relationships between the blood levels of NAD^+ and thiamine status parameters are significantly altered in female CMT patients, compared to healthy women. The therapy with thiamine and NR shifts these relationships towards the control ones, indicating metabolic normalization.

DISCUSSION

The molecular mechanisms of CMT development induced by mutations in *GDAP1* have been extensively studied in a number of independent laboratories, because in certain populations mutations in this protein are the fifth most frequent cause of this common hereditary motor and sensory neuropathy [2]. In our work, the mechanisms of GDAP1 dysfunction upon its L239F/A175P substitutions in a compound heterozygous carrier with the early development of CMT2K pathology are analyzed. Using the structure-function analysis of GDAP1, we show that the amino acid substitutions caused by these mutations, may affect the same hydrophobic-compound-binding region (Fig. 3). As the heterozygous substitutions in parents jointly influence the same GDAP1 binding function in the compound heterozygous child, the function becomes strongly perturbed, leading to early onset of the disease in the child in the absence of symptoms in the parents.

Cellular phenotypes associated with *GDAP1* mutations leading to the amino acid substitutions in the hydrophobic-compound-binding region are analyzed in the most relevant models, such as patients' motor neurons and fibroblasts (Table 1). According to the analysis of these data, a key common consequence of amino acid substitutions in this region is a dysfunction of the mitochondrial TCA cycle. Independent studies investigating the effects of the L239 and C240 substitutions in GDAP1 report increased PDH phosphorylation (and reduction of NADH production in the TCA cycle) and decreased activity of the NADH-oxidizing complex I, respectively (Table 1). We have therefore suggested that thiamine and NR, which are biosynthetic precursors of ThDP and NAD^+, both activating PDH and TCA cycle, should be useful in the treatment of the CMT2K patient with the compound heterozygous L239F/A175P substitution. ThDP (the coenzyme form of thiamine) activates PDH not only by saturating the enzyme active sites, but also by inhibiting PDH phosphorylation, since ThDP acts as an inhibitor of pyruvate dehydrogenase kinases (PDK) [50, 51]. It should be mentioned that increased PDH phosphorylation is associated with CMT not only upon substitutions in the hydrophobic-compound-binding region of GDAP1 (Table 1), but also in the case of upregulation of PDH phosphorylation by the activating mutation in PDK3 [58]. Moreover, inactivation of PDH due to a heterozygous mutation leading to the L138F substitution in the enzyme α-subunit causes demyelination, which is one of the characteristic features of CMT [59, 60]. It is worth noting that both GDAP1 [61, 62] and PDK isoenzyme 4 (PDK4) are involved in the dynamin-related protein 1 (DRP1)-mediated mitochondrial fragmentation [63]. That is, DRP1 interaction with the mitochondria is controlled by phosphorylation of the non-canonical PDK4 substrate septin 2 [63]. ThDP not only inhibits PDK [50, 51], but also reduces the activating phosphorylation of DRP1 at S616 [64], which promotes mitochondrial fragmentation. Hence, mitochondrial fragmentation depends on the action of PDK and ThDP on the phosphorylation of septin 2 and DRP1. These data provide independent evidence linking PDH phosphorylation to the observed disturbances in the mitochondrial dynamics in *GDAP1* mutants. It should be noted that PDKs exhibit tissue-specific expression. Expression of PDK4 in the nervous tissue is negligible under normal conditions. However, PDK4 may significantly increase in metabolic disorders [65]. Probably, the energy imbalance in *GDAP1* mutants activates PDK4 expression in the nervous tissue and/or muscles. Hence, the therapeutic action of thiamine as a precursor of ThDP in L239F/A175P-substituted GDAP1 and in other forms of CMT [40] may be an indicator of common disturbances in the PDH phosphorylation associated with CMT of different etiology. As discussed above, mitochondrial dysfunction and fragmentation, often observed in *GDAP1* mutations, may be a coupled effect of PDK upregulation.

When characterizing the therapeutic action of thiamine and NR, we have found that the increase

in the hand grip strength correlates more with the blood levels of ThDP than those of NAD^+ or TKT activity. However, a combined administration of thiamine and NR promotes metabolic normalization, expressed in the activating effect of ThDP on TKT and in the correlations between the blood levels of the thiamine status parameters (ThDP, holo-TKT activity) and NAD^+. At the same time, it should be kept in mind that the metabolism of NR and other NAD^+ precursors involves complex interactions between body tissues [66, 67]. Furthermore, available low-invasive blood tests used in clinical studies is not optimal for detecting an increase in the NAD^+ biosynthesis, since most NAD^+ is located in the mitochondria, which are absent in erythrocytes representing the major fraction of blood cells. For the same reason, whole-blood analysis is not appropriate for characterization of mitochondrial metabolism. The small changes in the blood levels of NAD^+, observed upon the intake of NR (Fig. 5), may be a consequence of the low NAD^+ content in this tissue. Nevertheless, the measured blood parameters, such as the TKT regulation by ThDP and the correlations between NAD^+, ThDP, and holo-TKT activity can be used as markers of metabolic changes in the entire body. In particular, comparison of these indicators and their relationships in the control and CMT group points to the metabolic normalization in the CMT2K patient treated with a combination of thiamine and NR. It is possible that an earlier administration of thiamine and NR could be more efficient, as slowing down the development of a pathology is more feasible than repairing already damaged system. This consideration justifies the metabolic correction therapy based on the early identification of CMT-causing mutations and biochemical mechanisms of their pathogenicity before the appearance of pronounced clinical symptoms and significant disability of patients.

Supplementary information

The online version contains supplementary material available at https://doi.org/10.1134/S0006297925601911.

Contributions

N.R.B. performed NAD^+ assays, analyzed published reports on phenotypes of *GDAP1* mutations and regulatory role of kinases, analyzed and visualized dynamics of the clinical parameters; A.A.E. performed structure-function analysis and visualization of GDAP1, analyzed published data of *in vitro* studies of GDAP1; O.N.S. performed ThDP and TKT activity assays; N.V.B. collected blood, performed NAD^+ assays, and curated the data; O.P.S. performed neurologic tests and clinical follow-up of the patient; V.I.B. developed the study concept, supervised the study, analyzed the results and literature, and wrote the manuscript. All authors discussed the results, read the paper, and agreed on the presented version of the paper.

Funding

This work was supported by the State Program AAAA-A19-119042590056-2.

Ethics approval and consent to participate

The study was approved by the Ethics Committee of Vladimirsky Moscow Regional Research and Clinical Institute (protocol no. 17, December 10, 2020). All the study participants provided voluntary informed consent. For the minor patient, the consent was provided by the mother.

Conflict of interest

The authors of this work declare that they have no conflicts of interest.

REFERENCES

1. Bunik, V. I. (2024) A challenging interplay between basic research, technologies and medical education to provide therapies based on disease mechanisms, *Front. Med. (Lausanne)*, **11**, 1464672, https://doi.org/10.3389/fmed.2024.1464672.
2. Dai, S., Zheng, J., Chen, Y., Zhu, J., Wang, X., Peng, Y., Luo, Y., Lin, T., Li, Y., Ma, M., Shi, Z., Meng, X., Sun, L., and Zhou, J. C. (2025) A cross-sectional survey on the health status of patients with Charcot-Marie-Tooth disease in a Chinese national patient group, *J. Neurol.*, **272**, 322, https://doi.org/10.1007/s00415-025-13063-7.
3. Cassereau, J., Chevrollier, A., Bonneau, D., Verny, C., Procaccio, V., Reynier, P., and Ferré, M. (2011) A locus-specific database for mutations in GDAP1 allows analysis of genotype-phenotype correlations in Charcot-Marie-Tooth diseases type 4A and 2K, *Orphanet J. Rare Dis.*, **6**, 87, https://doi.org/10.1186/1750-1172-6-87.
4. Kotov, S., Sidorova, O., and Borodataya, E. (2019) Mitochondrial disorders in neuromuscular pathology, *Neuromusc. Dis.*, **9**, 22-31, https://doi.org/10.17650/2222-8721-2019-9-3-22-31.
5. Niemann, A., Ruegg, M., La Padula, V., Schenone, A., and Suter, U. (2005) Ganglioside-induced differentiation associated protein 1 is a regulator of the mitochondrial network: new implications for Charcot-Marie-Tooth disease, *J. Cell Biol.*, **170**, 1067-1078, https://doi.org/10.1083/jcb.200507087.
6. Pakhrin, P. S., Xie, Y., Hu, Z., Li, X., Liu, L., Huang, S., Wang, B., Yang, Z., Zhang, J., Liu, X., Xia, K., Tang, B., and Zhang, R. (2018) Genotype-phenotype correlation and frequency of distribution in a cohort of Chinese Charcot-Marie-Tooth patients associated with GDAP1 mutations, *J. Neurol.*, **265**, 637-646, https://doi.org/10.1007/s00415-018-8743-9.

7. González-Sánchez, P., Satrústegui, J., Palau, F., and Del Arco, A. (2019) Calcium deregulation and mitochondrial bioenergetics in GDAP1-related CMT, *Int. J. Mol. Sci.*, **20**, 403, https://doi.org/10.3390/ijms20020403.
8. Cantarero, L., García-Vargas, G., Hoenicka, J., and Palau, F. (2023) Differential effects of Mendelian GDAP1 clinical variants on mitochondria-lysosome membrane contacts sites, *Biol. Open*, **12**, bio059707, https://doi.org/10.1242/bio.059707.
9. Xia, M., Zhang, Y., Jin, K., Lu, Z., Zeng, Z., and Xiong, W. (2019) Communication between mitochondria and other organelles: a brand-new perspective on mitochondria in cancer, *Cell Biosci.*, **9**, 27, https://doi.org/10.1186/s13578-019-0289-8.
10. Xin, B., Puffenberger, E., Nye, L., Wiznitzer, M., and Wang, H. (2008) A novel mutation in the GDAP1 gene is associated with autosomal recessive Charcot-Marie-Tooth disease in an Amish family, *Clin. Genet.*, **74**, 274-278, https://doi.org/10.1111/j.1399-0004.2008.01018.x.
11. Ortiz-Santiago, A., and Ramos, E. (2021) Childhood onset homozygous recessive GDAP1 (p.Pro231Leu) mutation in a 9-year-old puerto rican pediatric female with axonal Charcot-Marie-Tooth disease: a case report, *J. Pediatr. Rehabil. Med.*, **14**, 533-537, https://doi.org/10.3233/prm-200695.
12. Manzoor, U., Ali, A., Ali, S. L., Abdelkarem, O., Kanwal, S., Alotaibi, S. S., Baazeem, A., Baiduissenova, A., Yktiyarov, A., Hajar, A., and Olzhabay, A. (2023) Mutational screening of GDAP1 in dysphonia associated with Charcot-Marie-Tooth disease: clinical insights and phenotypic effects, *J. Genet. Eng. Biotechnol.*, **21**, 119, https://doi.org/10.1186/s43141-023-00568-9.
13. Vivar, C., and Avila, J. D. (2019) GDAP1-related Charcot-Marie-Tooth disease: additional evidence for the c.692C>T variant as a pathogenic mutation (P3.4-045), *Neurology*, **92**, P3.4-045, https://doi.org/10.1212/WNL.92.15_supplement.P3.4-045.
14. Wolf, C., Pouya, A., Bitar, S., Pfeiffer, A., Bueno, D., Rojas-Charry, L., Arndt, S., Gomez-Zepeda, D., Tenzer, S., Bello, F. D., Vianello, C., Ritz, S., Schwirz, J., Dobrindt, K., Peitz, M., Hanschmann, E. M., Mencke, P., Boussaad, I., Silies, M., Brüstle, O., et al. (2022) GDAP1 loss of function inhibits the mitochondrial pyruvate dehydrogenase complex by altering the actin cytoskeleton, *Commun. Biol.*, **5**, 541, https://doi.org/10.1038/s42003-022-03487-6.
15. Kabzińska, D., Strugalska-Cynowska, H., Kostera-Pruszczyk, A., Ryniewicz, B., Posmyk, R., Midro, A., Seeman, P., Báranková, L., Zimoń, M., Baets, J., Timmerman, V., Guergueltcheva, V., Tournev, I., Sarafov, S., De Jonghe, P., Jordanova, A., Hausmanowa-Petrusewicz, I., and Kochański, A. (2010) L239F founder mutation in GDAP1 is associated with a mild Charcot-Marie-Tooth type 4C4 (CMT4C4) phenotype, *Neurogenetics*, **11**, 357-366, https://doi.org/10.1007/s10048-010-0237-6.
16. Noack, R., Frede, S., Albrecht, P., Henke, N., Pfeiffer, A., Knoll, K., Dehmel, T., Meyer Zu Hörste, G., Stettner, M., Kieseier, B. C., Summer, H., Golz, S., Kochanski, A., Wiedau-Pazos, M., Arnold, S., Lewerenz, J., and Methner, A. (2012) Charcot-Marie-Tooth disease CMT4A: GDAP1 increases cellular glutathione and the mitochondrial membrane potential, *Hum. Mol. Genet.*, **21**, 150-162, https://doi.org/10.1093/hmg/ddr450.
17. Sutinen, A., Paffenholz, D., Nguyen, G. T. T., Ruskamo, S., Torda, A. E., and Kursula, P. (2023) Conserved intramolecular networks in GDAP1 are closely connected to CMT-linked mutations and protein stability, *PLoS One*, **18**, e0284532, https://doi.org/10.1371/journal.pone.0284532.
18. Marco, A., Cuesta, A., Pedrola, L., Palau, F., and Marín, I. (2004) Evolutionary and structural analyses of GDAP1, involved in Charcot-Marie-Tooth disease, characterize a novel class of glutathione transferase-related genes, *Mol. Biol. Evol.*, **21**, 176-187, https://doi.org/10.1093/molbev/msh013.
19. Googins, M. R., Woghiren-Afegbua, A. O., Calderon, M., St Croix, C. M., Kiselyov, K. I., and VanDemark, A. P. (2020) Structural and functional divergence of GDAP1 from the glutathione S-transferase superfamily, *FASEB J.*, **34**, 7192-7207, https://doi.org/10.1096/fj.202000110R.
20. Nguyen, G. T. T., Sutinen, A., Raasakka, A., Muruganandam, G., Loris, R., and Kursula, P. (2020) Structure of the complete dimeric human GDAP1 core domain provides insights into ligand binding and clustering of disease mutations, *Front. Mol. Biosci.*, **7**, 631232, https://doi.org/10.3389/fmolb.2020.631232.
21. Huber, N., Bieniossek, C., Wagner, K. M., Elsässer, H. P., Suter, U., Berger, I., and Niemann, A. (2016) Glutathione-conjugating and membrane-remodeling activity of GDAP1 relies on amphipathic C-terminal domain, *Sci. Rep.*, **6**, 36930, https://doi.org/10.1038/srep36930.
22. Cassereau, J., Chevrollier, A., Codron, P., Goizet, C., Gueguen, N., Verny, C., Reynier, P., Bonneau, D., Lenaers, G., and Procaccio, V. (2020) Oxidative stress contributes differentially to the pathophysiology of Charcot-Marie-Tooth disease type 2K, *Exp. Neurol.*, **323**, 113069, https://doi.org/10.1016/j.expneurol.2019.113069.
23. Pla-Martín, D., Rueda, C. B., Estela, A., Sánchez-Piris, M., González-Sánchez, P., Traba, J., de la Fuente, S., Scorrano, L., Renau-Piqueras, J., Alvarez, J., Satrústegui, J., and Palau, F. (2013) Silencing of the Charcot-Marie-Tooth disease-associated gene GDAP1 induces abnormal mitochondrial distribution and affects Ca^{2+} homeostasis by reducing store-operated Ca^{2+} entry, *Neurobiol. Dis.*, **55**, 140-151, https://doi.org/10.1016/j.nbd.2013.03.010.

24. Sutinen, A., Jones, N. C., Hoffmann, S. V., Ruskamo, S., and Kursula, P. (2023) Conformational analysis of membrane-proximal segments of GDAP1 in a lipidic environment using synchrotron radiation suggests a mode of assembly at the mitochondrial outer membrane, *Biophys. Chem.*, **303**, 107113, https://doi.org/10.1016/j.bpc.2023.107113.
25. Chen, Y., Zhu, J., Wang, M., Zhao, Q., Huang, C., Tarjibayeva, S., Wang, L., Sun, L., and Zhou, J. C. (2025) Advances and clues of nutritional adjuvant therapy for Charcot-Marie-Tooth disease, *J. Nutr.*, **155**, 3642-3653, https://doi.org/10.1016/j.tjnut.2025.09.026.
26. Gubler, C. J., Johnson, L. R., and Wittorf, J. H. (1970) Yeast transketolase (sedoheptulose-7-phosphate:d-glyceraldehyde-3-phosphate dihydroxyacetonetransferase, EC 2.2.1.1) assay of thiamine diphosphate, *Methods Enzymol.*, **18**, 120-125, https://doi.org/10.1016/0076-6879(71)18290-0.
27. Kochetov, G. A. (1980) *Practice Guidelines on Biochemistry* [in Russian], Vysshaya Shkola, Moscow.
28. Solovjeva, O. N. (2002) Isolation and properties of noncovalent complex of transketolase with RNA, *Biochemistry (Moscow)*, **67**, 667-671, https://doi.org/10.1023/a:1016198321838.
29. Tikhomirova, N. K., and Kochetov, G. A. (1990) Purification of transketolase from baker's yeast by an immunoadsorbent, *Biochem. Int.*, **22**, 31-36.
30. Solovjeva, O. N., Selivanov, V. A., Orlov, V. N., and Kochetov, G. A. (2019) Stages of the formation of nonequivalence of active centers of transketolase from baker's yeast, *Mol. Catal.*, **466**, 122-129, https://doi.org/10.1016/j.mcat.2019.01.00.
31. Heinrich, C. P., Noack, K., and Wiss, O. (1972) Chemical modification of tryptophan at the binding site of thiamine-pyrophosphate in transketolase from Baker's yeast, *Biochem. Biophys. Res. Commun.*, **49**, 1427-1432, https://doi.org/10.1016/0006-291x(72)90498-6.
32. Kim, M., Won, C. W., and Kim, M. (2018) Muscular grip strength normative values for a Korean population from the Korea National Health and Nutrition Examination Survey, 2014-2015, *PLoS One*, **13**, e0201275, https://doi.org/10.1371/journal.pone.0201275.
33. Harding, A. E., and Thomas, P. K. (1980) The clinical features of hereditary motor and sensory neuropathy types I and II, *Brain*, **103**, 259-280, https://doi.org/10.1093/brain/103.2.259.
34. Wong, S. L. (2016) Grip strength reference values for Canadians aged 6 to 79: Canadian Health Measures Survey, 2007 to 2013, *Health Rep.*, **27**, 3-10.
35. Jumper, J., Evans, R., Pritzel, A., Green, T., Figurnov, M., Ronneberger, O., Tunyasuvunakool, K., Bates, R., Žídek, A., Potapenko, A., Bridgland, A., Meyer, C., Kohl, S. A. A., Ballard, A. J., Cowie, A., Romera-Paredes, B., Nikolov, S., Jain, R., Adler, J., Back, T., et al. (2021) Highly accurate protein structure prediction with AlphaFold, *Nature*, **596**, 583-589, https://doi.org/10.1038/s41586-021-03819-2.
36. Maupetit, J., Derreumaux, P., and Tuffery, P. (2009) PEP-FOLD: an online resource for de novo peptide structure prediction, *Nucleic Acids Res.*, **37**, W498-W503, https://doi.org/10.1093/nar/gkp323.
37. DeLano, W. L., and Bromberg, S. (2004) PyMOL user's guide, *DeLano Scientific LLC*.
38. Svensson, E., and Häger-Ross, C. (2006) Hand function in Charcot Marie Tooth: test retest reliability of some measurements, *Clin. Rehabil.*, **20**, 896-908, https://doi.org/10.1177/0269215506072184.
39. Bohannon, R. W. (2017) Test-retest reliability of measurements of hand-grip strength obtained by dynamometry from older adults: a systematic review of research in the PubMed database, *J. Frailty Aging*, **6**, 83-87, https://doi.org/10.14283/jfa.2017.8.
40. Artiukhov, A. V., Solovjeva, O. N., Balashova, N. V., Sidorova, O. P., Graf, A. V., and Bunik, V. I. (2024) Pharmacological doses of thiamine benefit patients with the Charcot-Marie-Tooth neuropathy by changing thiamine diphosphate levels and affecting regulation of thiamine-dependent enzymes, *Biochemistry (Moscow)*, **89**, 1161-1182, https://doi.org/10.1134/S0006297924070010.
41. Balashova, N. V., Zavileyskiy, L. G., Artiukhov, A. V., Shaposhnikov, L. A., Sidorova, O. P., Tishkov, V. I., Tramonti, A., Pometun, A. A., and Bunik, V. I. (2022) Efficient assay and marker significance of NAD(+) in human blood, *Front. Med. (Lausanne)*, **9**, 886485, https://doi.org/10.3389/fmed.2022.886485.
42. Reimer, U., Scherer, G., Drewello, M., Kruber, S., Schutkowski, M., and Fischer, G. (1998) Side-chain effects on peptidyl-prolyl cis/trans isomerisation, *J. Mol. Biol.*, **279**, 449-460, https://doi.org/10.1006/jmbi.1998.1770.
43. Schmidpeter, P. A., Koch, J. R., and Schmid, F. X. (2015) Control of protein function by prolyl isomerization, *Biochim. Biophys. Acta*, **1850**, 1973-1982, https://doi.org/10.1016/j.bbagen.2014.12.019.
44. Ammar, N., Nelis, E., Merlini, L., Barisić, N., Amouri, R., Ceuterick, C., Martin, J. J., Timmerman, V., Hentati, F., and De Jonghe, P. (2003) Identification of novel GDAP1 mutations causing autosomal recessive Charcot-Marie-Tooth disease, *Neuromuscul. Disord.*, **13**, 720-728, https://doi.org/10.1016/s0960-8966(03)00093-2.
45. Baránková, L., Vyhnálková, E., Züchner, S., Mazanec, R., Sakmaryová, I., Vondrácek, P., Merlini, L., Bojar, M., Nelis, E., De Jonghe, P., and Seeman, P. (2007) GDAP1 mutations in Czech families with early-onset CMT, *Neuromuscul. Disord.*, **17**, 482-489, https://doi.org/10.1016/j.nmd.2007.02.010.
46. Auer-Grumbach, M., Fischer, C., Papić, L., John, E., Plecko, B., Bittner, R. E., Bernert, G., Pieber, T. R., Miltenberger, G., Schwarz, R., Windpassinger, C., Grill, F., Timmerman, V., Speicher, M. R., and Janecke, A. R. (2008) Two novel mutations in the GDAP1

and PRX genes in early onset Charcot-Marie-Tooth syndrome, *Neuropediatrics*, **39**, 33-38, https://doi.org/10.1055/s-2008-1077085.

47. Moroni, I., Morbin, M., Milani, M., Ciano, C., Bugiani, M., Pagliano, E., Cavallaro, T., Pareyson, D., and Taroni, F. (2009) Novel mutations in the GDAP1 gene in patients affected with early-onset axonal Charcot-Marie-Tooth type 4A, *Neuromuscul. Disord.*, **19**, 476-480, https://doi.org/10.1016/j.nmd.2009.04.014.
48. Rougeot, C., Chabrier, S., Camdessanche, J. P., Prieur, F., d'Anjou, M. C., and Latour, P. (2008) Clinical, electrophysiological and genetic studies of two families with mutations in the GDAP1 gene, *Neuropediatrics*, **39**, 184-187, https://doi.org/10.1055/s-0028-1085467.
49. Binięda, K., Rzepnikowska, W., Kolakowski, D., Kaminska, J., Szczepankiewicz, A. A., Nieznańska, H., Kochański, A., and Kabzińska, D. (2021) Mutations in GDAP1 influence structure and function of the trans-Golgi network, *Int. J. Mol. Sci.*, **22**, 914, https://doi.org/10.3390/ijms22020914.
50. Cassereau, J., Chevrollier, A., Gueguen, N., Malinge, M. C., Letournel, F., Nicolas, G., Richard, L., Ferre, M., Verny, C., Dubas, F., Procaccio, V., Amati-Bonneau, P., Bonneau, D., and Reynier, P. (2009) Mitochondrial complex I deficiency in GDAP1-related autosomal dominant Charcot-Marie-Tooth disease (CMT2K), *Neurogenetics*, **10**, 145-150, https://doi.org/10.1007/s10048-008-0166-9.
51. Van den Bossche, D., Schiettecatte, J., Vekens, E., De Smet, D., Gorus, F. K., and Martens, G. A. (2012) Enzymatic pyruvate measurement by Cobas 6000 open channel assay, *Clin. Lab.*, **58**, 1091-1095.
52. Bunik, V. (2023) The therapeutic potential of vitamins B1, B3 and B6 in Charcot-Marie-Tooth disease with the compromised status of vitamin-dependent processes, *Biology (Basel)*, **12**, 897, https://doi.org/10.3390/biology12070897.
53. Jonus, H. C., Byrnes, C. C., Kim, J., Valle, M. L., Bartlett, M. G., Said, H. M., and Zastre, J. A. (2020) Thiamine mimetics sulbutiamine and benfotiamine as a nutraceutical approach to anticancer therapy, *Biomed. Pharmacother.*, **121**, 109648, https://doi.org/10.1016/j.biopha.2019.109648.
54. Pawlosky, R., Demarest, T. G., King, M. T., Estrada, D., Veech, R. L., and Bohr, V. A. (2025) Effect of dietary ketosis and nicotinamide riboside on hippocampal krebs cycle Intermediates and mitochondrial energetics in a DNA repair-deficient 3xTg/POLβ(+/–) Alzheimer disease mouse model, *J. Neurochem.*, **169**, e16295, https://doi.org/10.1111/jnc.16295.
55. Schaefer, P. M., Huang, J., Butic, A., Perry, C., Yardeni, T., Tan, W., Morrow, R., Baur, J. A., and Wallace, D. C. (2022) Nicotinamide riboside alleviates exercise intolerance in ANT1-deficient mice, *Mol. Metab.*, **64**, 101560, https://doi.org/10.1016/j.molmet.2022.101560.
56. Ahmadi, A., Begue, G., Valencia, A. P., Norman, J. E., Lidgard, B., Bennett, B. J., Van Doren, M. P., Marcinek, D. J., Fan, S., Prince, D. K., Gamboa, J., Himmelfarb, J., de Boer, I. H., Kestenbaum, B. R., and Roshanravan, B. (2023) Randomized crossover clinical trial of coenzyme Q10 and nicotinamide riboside in chronic kidney disease, *JCI Insight*, **8**, e167274, https://doi.org/10.1172/jci.insight.167274.
57. Kropotov, A., Kulikova, V., Nerinovski, K., Yakimov, A., Svetlova, M., Solovjeva, L., Sudnitsyna, J., Migaud, M. E., Khodorkovskiy, M., Ziegler, M., and Nikiforov, A. (2021) Equilibrative nucleoside transporters mediate the import of nicotinamide riboside and nicotinic acid riboside into human cells, *Int. J. Mol. Sci.*, **22**, 1391, https://doi.org/10.3390/ijms22031391.
58. Overton, E., Emelyanova, A., and Bunik, V. I. (2025) Thiamine, gastrointestinal beriberi and acetylcholine signaling, *Front. Nutr.*, **12**, 1541054, https://doi.org/10.3389/fnut.2025.1541054.
59. Ailabouni, A. S., Vijaywargi, G., Subash, S., Singh, D. K., Gaborik, Z., and Prasad, B. (2025) Is N1-methylnicotinamide a good organic cation transporter 2 (OCT2) biomarker? *Metabolites*, **15**, 80, https://doi.org/10.3390/metabo15020080.
60. Perez-Siles, G., Cutrupi, A., Ellis, M., Screnci, R., Mao, D., Uesugi, M., Yiu, E. M., Ryan, M. M., Choi, B. O., Nicholson, G., and Kennerson, M. L. (2020) Energy metabolism and mitochondrial defects in X-linked Charcot-Marie-Tooth (CMTX6) iPSC-derived motor neurons with the p.R158H PDK3 mutation, *Sci. Rep.*, **10**, 9262, https://doi.org/10.1038/s41598-020-66266-5.
61. Singhi, P., De Meirleir, L., Lissens, W., Singhi, S., and Saini, A. G. (2013) Pyruvate dehydrogenase-e1α deficiency presenting as recurrent demyelination: an unusual presentation and a novel mutation, *JIMD Rep.*, **10**, 107-111, https://doi.org/10.1007/8904_2012_211.
62. Bonne, G., Benelli, C., De Meirleir, L., Lissens, W., Chaussain, M., Diry, M., Clot, J. P., Ponsot, G., Geoffroy, V., Leroux, J. P., and Marsac, C. (1993) E1 pyruvate dehydrogenase deficiency in a child with motor neuropathy, *Pediatr. Res.*, **33**, 284-288, https://doi.org/10.1203/00006450-199303000-00016.
63. Huber, N., Guimaraes, S., Schrader, M., Suter, U., and Niemann, A. (2013) Charcot-Marie-Tooth disease-associated mutants of GDAP1 dissociate its roles in peroxisomal and mitochondrial fission, *EMBO Rep.*, **14**, 545-552, https://doi.org/10.1038/embor.2013.56.
64. Niemann, A., Wagner, K. M., Ruegg, M., and Suter, U. (2009) GDAP1 mutations differ in their effects on mitochondrial dynamics and apoptosis depending on the mode of inheritance, *Neurobiol. Dis.*, **36**, 509-520, https://doi.org/10.1016/j.nbd.2009.09.011.
65. Thoudam, T., Chanda, D., Sinam, I. S., Kim, B. G., Kim, M. J., Oh, C. J., Lee, J. Y., Kim, M. J., Park, S. Y., Lee, S. Y., Jung, M. K., Mun, J. Y., Harris, R. A., Ishihara, N.,

Jeon, J. H., and Lee, I. K. (2022) Noncanonical PDK4 action alters mitochondrial dynamics to affect the cellular respiratory status, *Proc. Natl. Acad. Sci. USA*, **119**, e2120157119, https://doi.org/10.1073/pnas.2120157119.

66. Yamada, Y., Kusakari, Y., Akaoka, M., Watanabe, M., Tanihata, J., Nishioka, N., Bochimoto, H., Akaike, T., Tachibana, T., and Minamisawa, S. (2021) Thiamine treatment preserves cardiac function against ischemia injury via maintaining mitochondrial size and ATP levels, *J. Appl. Physiol.*, **130**, 26-35, https://doi.org/10.1152/japplphysiol.00578.2020.
67. Klyuyeva, A., Tuganova, A., Kedishvili, N., and Popov, K. M. (2019) Tissue-specific kinase expression and activity regulate flux through the pyruvate dehydrogenase complex, *J. Biol. Chem.*, **294**, 838-851, https://doi.org/10.1074/jbc.RA118.006433.
68. Kropotov, A., Kulikova, V., Solovjeva, L., Yakimov, A., Nerinovski, K., Svetlova, M., Sudnitsyna, J., Plusnina, A., Antipova, M., Khodorkovskiy, M., Migaud, M. E., Gambaryan, S., Ziegler, M., and Nikiforov, A. (2022) Purine nucleoside phosphorylase controls nicotinamide riboside metabolism in mammalian cells, *J. Biol. Chem.*, **298**, 102615, https://doi.org/10.1016/j.jbc.2022.102615.
69. Song, W. S., Shen, X., Du, K., Ramirez, C. B., Park, S. H., Cao, Y., Le, J., Bae, H., Kim, J., Chun, Y., Khong, N. J., Kim, M., Jung, S., Choi, W., Lopez, M. L., Said, Z., Song, Z., Lee, S. G., Nicholas, D., Sasaki, Y., et al. (2025) Nicotinic acid riboside maintains NAD(+) homeostasis and ameliorates aging-associated NAD(+) decline, *Cell Metab.*, **37**, 1616-1618, https://doi.org/10.1016/j.cmet.2025.05.004.